The Journal of Experimental Biology 215, 141-151
© 2012. Published by The Company of Biologists Ltd
doi:10.1242/jeb.060541

RESEARCH ARTICLE

Earliest ciliary swimming effects vertical transport of planktonic embryos in turbulence and shear flow

Kathryn A. McDonald

Friday Harbor Laboratories and Department of Biology, University of Washington, 620 University Road, Friday Harbor, WA 98250-9299, USA

Present address: Smithsonian Tropical Research Institute, Apartado Postal 0834-03092, Balboa Ancón, República de Panamá (kamcdon@post.harvard.edu)

Accepted 7 September 2011

SUMMARY

Eggs released by broadcast-spawning marine invertebrates are often negatively buoyant. Blastulae and gastrulae of these species are commonly motile, with passive stability that leads to upward swimming in still water. The earliest occurrence of swimming in developing embryos of diverse invertebrates may therefore permit vertical migration in nature. I used turbulent and laminar shear flows to investigate: (1) the speed and direction of transport of non-motile and newly swimming stages of the echinoids *Dendraster excentricus* and *Strongylocentrotus purpuratus* in turbulence, and (2) the limit of stable vertical orientation in swimming blastulae of *D. excentricus*. Swimming contributed significantly to the rate of upward transport of *D. excentricus* in turbulence experiments where the kinetic energy dissipation rate (ε) was ~10^{-2} cm^2 s^{-3}. However, swimming significantly reduced the rate of upward transport of *S. purpuratus* blastulae in turbulence, suggesting that passively stable swimmers of this species were turned from the vertical, crossed flow-lines, and migrated into downwelling. Observations of swimming in laminar shear indicate that *D. excentricus* swimming blastulae maintain a vertical orientation until shear approaches 0.26 s^{-1}, equivalent to sub-microscale shear in turbulence where ε is ~10^{-3} cm^2 s^{-3}. Swimming speeds of *D. excentricus* showed an unexpected dependence on shear, indicating that greater shear (within limits) can enhance speed of ciliary swimming. In *D. excentricus*, swimming by newly hatched blastulae should support upward migration in turbulence characteristic of coastal surface waters, whereas species differences in passive stability and swimming responses to shear may lead to differences in vertical transport and subsequent dispersal.

Key words: embryo, blastula, swimming, vertical migration, turbulence, shear, *Dendraster excentricus.*

INTRODUCTION

Behavioral regulation of vertical transport is broadly important for zooplankters because water-column resources and risks are vertically structured. For invertebrate larvae, depth regulation is likely to have consequences for development time and for onshore and offshore transport. Development times are particularly responsive to temperature, which varies with depth and intensity of mixing, and to food availability, which is affected by the concentration of phytoplankton into horizontal thin layers and surface blooms (e.g. Bearon et al., 2006; Kamykowski and Yamazaki, 1997; Marra, 1980; Podolsky, 1995; Prézelin, 1992; Strathmann, 1987). Aspects of larval form and swimming behavior could interact with the fluid environment to optimize development time against risks from exposure to ultraviolet radiation and predator aggregations. By regulating their vertical position, larvae can also limit or direct their horizontal dispersal (e.g. Marta-Almeida et al., 2006; Poulin et al., 2002; Shanks, 1985; Verdier-Bonnet et al., 1997).

The morphology of echinoid plutei (Clay and Grünbaum, 2011) and swimming behavior of plutei, gastropod veligers and crab larvae (Chan and Grünbaum, 2010; Fuchs et al., 2004) show adaptations for control of vertical transport and selection of settlement habitat. Pluteus larvae have a skeletonized posterior and paired, ciliated anterior arms that provide swimming thrust. Echinopluteus arm-length ratios and arm conformations point to evolutionary compromises between swimming speed and stability of larvae, which enable a degree of depth control in a landscape of fluid shear (Clay and Grünbaum, 2011; Grünbaum and Strathmann, 2003). Gastropod veligers are shelled larvae with paired, retractable tissue flaps (the velar lobes) that are equipped with a marginal band or bands of cilia. Veligers' behavioral responses to fluid shear can differ among species and among developmental stages, which leads to differences in net upward transport under similar environmental conditions; direct or indirect responses to shear (i.e. responses mediated by a dissolved cues) may result in selection of settlement habitats that meet juvenile or adult tolerances (e.g. Fuchs et al., 2004; Fuchs et al., 2007; Fuchs et al., 2010; Koehl et al., 2007). The diel vertical migrations (DVMs) undertaken by larvae of many gastropods, polychaete worms and brachyuran crabs also represent behavioral adaptations for control of vertical transport, often driven by predation pressure (e.g. Bollens et al., 1992; Bollens et al., 2011; Lampert, 1989). This iterative pattern of daily migration can have direct consequences for the direction and extent of horizontal advection; for instance, DVM can reduce the offshore dispersion of larvae from large-scale upwelling and downwelling events (Garland et al., 2002; Marta-Almeida et al., 2006; Poulin et al., 2002; Shanks, 1985). Active depth control is clearly an important feature of successful development for many long-lived larvae at different stages in their tenure in the plankton.

For broadcast spawners, vertical migration may be equally important during earliest development, as unprotected eggs are

released into epibenthic environments where predators can occur at high numeric density (Allen and McAlister, 2007; Morgan, 1990; Strathmann, 1982). The excess density (i.e. the density difference from ambient seawater; $kg\,m^{-3}$) of eggs and embryos is one factor affecting the rate and direction of transport during embryogenesis (Coombs et al., 1985; Kelman and Emlet, 1999; McDonald and Grünbaum, 2010; Medeiros-Bergen et al., 1995; Sundby, 1983; Sundby, 1997; Young and Cameron, 1987). Embryos and early larvae could also regulate their vertical transport through active adjustment of buoyancy (McDonald, 2004; Childress and Nygaard, 1974; Visser and Jonasdóttir, 1999), and taxis and swimming behaviors (e.g. Bearon et al., 2004; Chan and Grünbaum, 2010; Clay and Grünbaum, 2010; Emlet, 1986; Fuchs et al., 2004; Gallager, 1993; Grünbaum and Strathmann, 2003; Kamykowski and Yamazaki, 1997; McDonald, 2004; Metaxas, 2001; Seuront et al., 2004; Yamazaki and Squires, 1996; Young, 1995; Young and Chia, 1987).

Although positive buoyancy and active density regulation are not unknown among invertebrate eggs and embryos, the development of broadcast spawners commonly involves a transition to ciliary swimming before or during the time of gastrulation. Embryos of many different broadcast spawners develop rapidly to swimming and have a passively maintained upward orientation (Staver and Strathmann, 2002) that could enable migration away from the benthos. Ciliated early embryos are generally quite small (<0.3 mm diameter) and are weak swimmers, capable of maximum upward speeds in the range of $1.5–6.0\times10^{-2}\,cm\,s^{-1}$ (e.g. McDonald and Grünbaum, 2010). However, these speeds are similar in magnitude to mean sub-microscale flow velocities in moderate oceanic turbulence (10^{-3} to $10^{-5}\,cm^2\,s^{-3}$; Table 1). Closely related species can differ in upward swimming speeds at the time of first motility, and in the magnitude of change in velocity that accompanies the transition from passive sinking to upward swimming (McDonald and Grünbaum, 2010; McDonald, 2004). It is possible, then, that species differ in their capacity for migration at these early stages, and in the net impact of early motility on their dispersal.

The effectiveness of upward swimming for vertical transport depends upon the coupling between a swimmer's behavior and morphology and the physical characteristics of its fluid environment. Early embryos are amenable to quantitative predictions about swimming speed because of their small sizes, simple shapes and slow swimming speeds (McDonald and Grünbaum, 2010). However, upward swimming speeds alone are unlikely to predict relative rates and patterns of vertical transport in nature. A swimmer's stability, or resistance to turning, must also be taken into account. Swimming speed and passive stability may both show dependence upon embryonic size (McDonald, 2004; McDonald and Grünbaum, 2010). Passive stability, the component of overall swimming stability that derives from physical features of the embryo (e.g. Mogami et al., 2001), is otherwise determined by shape, mass and the distribution of mass. In an echinoderm coeloblastula, for instance, mass is concentrated at the embryonic vegetal pole, and the center of buoyancy is displaced anteriorly (in the direction of the animal pole); this is the basis of the blastula's passive stability moment, $\mathbf{M_B}$:

$$\mathbf{M_B} \propto r\,[\rho \boldsymbol{g} r^3], \tag{1}$$

where ρ represents embryonic excess density, $\boldsymbol{g}$ is gravitational acceleration and r^3 is volume, the cube of characteristic length r. The passive stability moment is thus proportional to the product of body force with a moment arm defined by the separation between the centers of gravity and buoyancy. It is reasonable to assume isometry among early blastulae of different echinoid species, so this moment arm can be taken as proportional to radius (r). Increasing the distance between the centers of gravity and buoyancy will therefore increase stability. If one assumes both isometry and equal density, larger embryos are inherently more stable than smaller embryos, though a larger coeloblastula may swim more slowly than a smaller one (Grünbaum and Strathmann, 2003; McDonald, 2004).

Environmental characteristics will also determine the effectiveness of upward swimming for vertical transport. Published measures for ε, the rate of kinetic energy dissipation in turbulence, vary with depth, distance from shore and conditions of the tide, currents and surface waters (e.g. Gargett, 1984; George et al., 1994; McKenzie and Leggett, 1993; Oakey and Elliott, 1982). As ε increases, the size-scale of the smallest eddies diminishes, and mean velocity within the smallest eddies increases; sub-microscale shear rate increases proportionally. High values of ε in surface-mixed layers of the open ocean are frequently reported as $10^{-2}–10^{-3}\,cm^2\,s^{-3}$, at least one order of magnitude lower than turbulence dissipation rates commonly measured in coastal areas (e.g. George et al., 1994; McKenzie and Leggett, 1993; Oakey and Elliott, 1982). Only in strong coastal turbulence ($\varepsilon\geq10^{-1}\,cm^2\,s^{-3}$) will the Kolmogorov length η, or microscale of turbulence, approach the size of early-stage planktonic embryos (Table 1). Sub-microscale conditions of shear should in general comprise an embryo's experience of flow. The behavioral transport of embryos in nature will depend upon their resistance to turning in shear.

A velocity differential – in other words, shear flow – exerts a force on a passively stable swimmer in proportion to the embryo's size:

$$\mathbf{M_S} \propto r\,(\mu r^2 \boldsymbol{\nabla}\mathbf{U}), \tag{2}$$

where μ is the dynamic viscosity of the medium ($kg\,m^{-1}\,s^{-1}$), $\mathbf{U}$ is flow velocity and r is again the characteristic length or radius of the embryo. If this flow-derived stability moment $\mathbf{M_S}$ is greater than the moment derived from body force ($\mathbf{M_B}$), the anterior (or upward) pole of the embryo will tend to rotate towards lesser

Table 1. Kolmogorov scales, at a kinematic viscosity of $10^{-6}\,m^2\,s^{-1}$

ε ($cm^2\,s^{-3}$)	η (cm)	v ($cm\,s^{-1}$)	Shear (s^{-1}; v/η)
10^{-1}	5.62×10^{-2}	1.78×10^{-1}	3.17
10^{-2}	1.0×10^{-1}	1.0×10^{-1}	1.0
10^{-3}	1.78×10^{-1}	5.62×10^{-2}	3.16×10^{-1}
10^{-4}	3.16×10^{-1}	3.16×10^{-2}	1.0×10^{-1}
10^{-5}	5.62×10^{-1}	1.78×10^{-2}	3.16×10^{-2}

Data are from Yamazaki et al. (Yamazaki et al., 2002).

ε, rate of turbulent kinetic energy dissipation; η, Kolmogorov length, or microscale of turbulence v, Kolmogorov velocity.

Shear experiments in this study utilized shears in the range of 2×10^{-1} to 5×10^{-1}, which corresponds to $\varepsilon\approx10^{-3}\,cm^2\,s^3$; turbulence experiments were conducted under conditions where $\varepsilon\approx10^{-2}\,cm^2\,s^3$.

upwelling in a flow-field (Grünbaum and Strathmann, 2003). A portion of the swimming velocity once directed vertically is then deflected horizontally. Passively stable swimmers in shear therefore have the potential to cross flow-lines into downwelling, turning upward migration into downward transport (Clay and Grünbaum, 2010; Grünbaum and Strathmann, 2003).

Faster swimming with reduced stability could simply mean that embryos are more readily transported downwards; in highly turbulent conditions, larger, slower-swimming embryos may be more effective at upward migration. Rather than taking greater upward swimming speed to indicate greater capability for migration, embryonic speed and stability will likely interact with turbulence to define a species' behavioral contribution to transport. Predicting the effects of early motility on the planktonic transport and distribution of early developmental stages therefore requires knowledge of their stability and swimming performance in shear.

In this study I compared the effects of swimming on the transport of blastulae in turbulent flow, and used shear flow to determine the limit of passive stability in swimming blastulae of one species. In laboratory experiments with turbulence, I used blastulae of the sand dollar *Dendraster excentricus* (Eschscholtz 1831) (Echinoidea: Clypeasteroida) and the sea urchin *Strongylocentrotus purpuratus* (Stimpson 1857) (Echinoidea: Euechinoida). Eggs of both species sink (i.e. are negatively buoyant). Upward swimming begins after the previously non-motile blastulae hatch from their fertilization envelopes. Blastulae of *S. purpuratus* are smaller in size than *D. excentricus* blastulae, but have approximately twice the excess density of the larger species (McDonald and Grünbaum, 2010). *Strongylocentrotus purpuratus* embryos also swim significantly faster at the time of hatching (McDonald, 2004). This first set of experiments utilized an oscillating grid-stirred turbulence tank (Brumley and Jirka, 1987; Hill et al., 1992). Transport velocities in turbulence were measured for embryos from one cross, both before and after hatching, with background velocity subtracted in order to examine effects of embryonic sinking and swimming on transport.

In the second group of experiments, swimming velocities of newly hatched *D. excentricus* blastulae were quantified in different laminar shear fields. Results for total speed and upward velocity of embryos in turbulence, and for speed, orientation and swimming responses in constant and changing shear fields, are discussed with a focus on implications for migration in nature.

MATERIALS AND METHODS

Embryonic transport in turbulence

To measure the effect of acquisition of motility on the speed and direction of embryonic transport in turbulence, I video-recorded the motion of unhatched (non-motile) and newly hatched (swimming) blastulae of *D. excentricus* and *S. purpuratus* in a grid-stirred turbulence tank, originally constructed for Hill et al. (Hill et al., 1992) and described therein. The Plexiglas® tank has approximate dimensions of 50×50×40 cm. The moving grid, which oscillates vertically, is driven by a center post attached to a motor-driven wheel, so that changing the attachment point of the post changes the amplitude of each grid-stroke. Adjusting power to the motor changes the stroke frequency. In this study, amplitude was set to 4.0 cm and the frequency to 2.5 s^{-1} to generate ε on the order of 10^{-2} $cm^2 s^{-3}$ (10^{-6} W kg^{-1}) at a height of 28.5 cm from the tank bottom, or 20.5 cm from the grid-stroke midpoint (Hill et al., 1992).

Recordings were made with a digital video camera (Canon model GL2, Glazer's Cameras, Seattle, WA, USA); a digital zoom feature permitted observation of an approximately 2×3 mm window at the tank center with a depth-of-field <2.0 mm. The face of the tank opposite the camera was backlit through a narrow window of translucent white Plexiglas® and otherwise obscured. The other tank faces were fully obscured to aid contrast. The camera was not moved during a trial. Prior to each trial, distance was calibrated with a scaled rod projecting from the center post downward into the tank.

Dendraster excentricus and *S. purpuratus* embryos were cultured by standard methods (Strathmann, 1987). Video-recording of each species comprised a separate trial. The experimental treatment was the embryonic stage: in each trial, one recording was made with non-motile blastulae prior to the time of hatching, and a second recording was made with swimming blastulae 1 h after completion of hatching. Prior to each trial, the tank was filled with bag-filtered (~10 μm pore size) seawater. Unhatched blastulae were transferred at very high density to the tank with the grid in oscillation. Each recording lasted 45–50 min. When the first recording was complete, I drained the tank and inspected embryos with a compound microscope to make certain that they were still intact and unhatched. The tank was then rinsed, drained again and refilled when another batch of blastulae from the same culture hatched and begun upward swimming. Tank temperature was measured before and after each recording, with an increase in temperature <0.5°C; the fluid volume was great enough to buffer against an undesirable temperature increase.

Sampling and analysis of turbulence experiments

Each 45–50 min recording was sampled at set intervals, and each sample was 30 s in duration. For *S. purpuratus*, five intervals were sampled in each embryonic stage treatment, with 150 embryos tracked through each sample; for *D. excentricus*, I increased the number of sampled intervals to seven, with 120 embryos tracked through each sample (Table 2). Samples were captured at 30 frames s^{-1} and individual frames were reassembled into stacks in

Table 2. Rates of upward transport in turbulence, $\varepsilon \approx 10^{-2}$ $cm^2 s^{-3}$

Species	Vertical velocity[a] ($mm s^{-1}$)	Total speed[a] ($mm s^{-1}$)	No. embryos (analyzed, total)	Sampling interval (s)	No. samples (analyzed, total)	No. embryos per sample
Strongylocentrotus purpuratus						
Unhatched	2.46±2.36	2.94±2.01	600, 750	30	4, 5	150
Swimming	1.48±2.51	3.26±2.01	600, 750	30	4, 5	150
Dendraster excentricus						
Unhatched	2.70±4.83	5.85±3.42	720, 840	30	6, 7	120
Swimming	3.81±3.57	5.73±2.97	720, 840	30	6, 7	120

Velocity and speed data are presented as means ± s.d.

[a]Significance for tests of performance by stage are as follows: *S. purpuratus*, vertical velocity, $P<0.001$ (two-tailed *t*-test, unequal variance); total speed, $P=0.011$ (two-tailed *t*-test, equal variance); *D. excentricus*, vertical velocity, $P<0.001$ (two-tailed *t*-test, unequal variance); total speed, $P=0.465$ (two-tailed *t*-test, unequal variance).

ImageJ (available as freeware; National Institutes of Health, Bethesda, MD, USA). Rectangular coordinates of individual embryos were saved at the time of their entry into the field of view and their exit. This enabled the automated calculation of a linearized trajectory and, therefore, velocity for each embryo over the time interval of observation. Once these individual trajectories had been calculated, I calculated and plotted a mean angle (direction) of embryo motion for each sample within a treatment. I used the Watson–Williams two-sample procedure (Zar, 1999) to test for differences in transport direction between unhatched (non-motile) and swimming treatments for each species.

I elected to discard one sampled interval from each treatment (unhatched and swimming) before testing for the effects of developmental stage on transport velocity. One sample from the unhatched treatment in both species' trials showed an atypical mean angle, which did not result from stage-related differences in embryonic performance but rather from a transient change in ambient flow velocity. It was acceptable to retain these data in the mean angle analysis, for reasons that will be discussed, but including them in the analysis of vertical velocity would have increased the likelihood of detecting an effect of swimming. Discarding the anomalous sample and another from the swimming treatment was the most conservative choice; I removed the corresponding time sample from the swimming treatment in each species trial.

Speeds of embryonic transport were not compared between trials (i.e. between species). Given differences in species' swimming performance measured in still water (McDonald, 2004), such comparisons would have been interesting. However, turbulence was not isotropic at the scale of these observations: a variable upwelling predominated in recordings. A slight change in camera position meant that patterns of upwelling observed in the first trial were different from those in the second.

Embryonic transport in shear

To determine the limit of passive stability in newly swimming *D. excentricus* blastulae, I quantified swimming speed and orientation in laminar vertical shear of varying magnitude. An advection chamber was constructed from two Nalgene™ tissue-culture flasks affixed upright to an acrylic base (Fig. 1). For each flask, identical outflow and inflow ports were inserted in the cap and the bottom rear wall, respectively. A black acrylic strip was cemented to the rear side of the space, and a clear piece to the front, leaving the top open. The interior chamber height was 5.2 cm, its depth 4.9 cm, and the separation between flasks 0.7 cm. To induce vertical circulation and the formation of a velocity gradient (laminar shear) in seawater within the intervening chamber, water was pumped into the flasks at the bottom and out at the top; temperature and flow for each side were separately regulated with recirculating heating/cooling baths, with one side maintained at higher temperature and the other at lower temperature. The four temperature intervals used in the first study (as measured by bath internal sensors) are reported in Table 3.

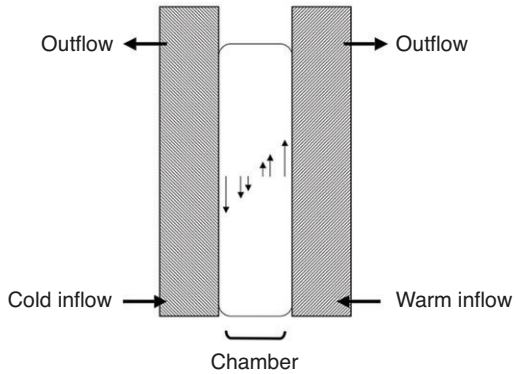

Fig. 1. Diagram of the convection chamber used to generate laminar shear for experiments with swimming *Dendraster excentricus* blastulae. Temperature separation across the seawater-filled central chamber is maintained by circulation of heated water through the right chamber and cooled water through the left. The direction of circulation within the chamber is indicated.

Dendraster excentricus embryos were cultured to hatching at ambient seawater temperatures (11–13°C). Eight sequential inseminations were used, so that batches of embryos reached hatching at staggered times. Once the chamber had been filled with 0.45-μm filtered seawater, the bath temperature controls were set and the flasks were allowed to come to temperature. A small number of newly hatched blastulae were then added to the chamber. The movement of embryos circulating through the chamber at a height of 2.0 cm was recorded with a CCD video camera and zoom macro lens, with analog output digitally converted and captured at 30 frames s^{-1}. The camera was not shifted between trials; instead, the chamber was drained, rinsed and refilled in position. The bath temperatures were then reset to the new interval, and the process repeated. Passive tracers (20 μm polystyrene beads) were recorded separately to establish background flow at each interval. Each interval was repeated twice in the same experiment, and the results for each were pooled.

A second, larger chamber was subsequently built to observe embryonic swimming in similar shear conditions, but farther from the uncharacterized shear environment of the chamber top and bottom. The new chamber was 14.0 cm in height, 10.3 cm in depth and 1.0 cm in breadth. Recordings were made at a height of 7.0 cm from the bottom. As before, vertical shear flow was induced by temperature separation, but the greater breadth of this second chamber resulted in different, non-linear shear profiles (Table 3). In this second experiment I used a Teflon™-coated type-T flexible implantable thermocouple (ThermoWorks, Salt Lake City, UT, USA; tip diameter approximately 500 μm) and a digital thermometer to measure temperature across the breadth of the chamber, and at varying height, with a small rack-and-pinion manipulator. Temperature measures were made subsequent to experiments with swimming embryos. These measures indicated that the majority of heat exchange occurred in close proximity to the chamber walls. Across the remainder of the cell, a breadth greater than the horizontal extent of the recording window, shear was not associated with a temperature gradient.

Sampling and analysis of shear experiments

Ambient flow velocities for each temperature interval/shear treatment were determined by measuring vertical speeds of near-neutrally buoyant polystyrene tracer beads. These cross-chamber profiles of tracer speed also indicated the extent of wall effects in each shear treatment, so that a horizontal window could be chosen to preclude wall effects. Regressions for ambient flow velocity allowed subtraction of ambient flow from embryonic vertical speed at any x-position. Once corrected for background flow, total speed was calculated for each embryo over short intervals, in this case 1-s time steps, and 'instantaneous' orientation was determined from the ratio of x- and y-displacement over each 1-s interval. For each embryo in a shear treatment, 15 to 35 s of data were collected and then subsampled, so that that each embryo was equally represented in analyses of performance.

Table 3. Shear characteristics from regression of 20-μm tracer particles

Treatment	No. embryos, observations	Treatment interval (°C)	Regression equation for background flow	R^2	x (cm)
Experiment 1: linear shear					
1	25, 110	10.0–13.0	y=0.2291x–0.0038	0.9905	–0.20<x<0.20
2	20, 99	10.0–14.0	y=0.2378x–0.0089	0.9838	–0.20<x<0.20
3	14, 69	9.5–14.5	y=0.2478x–0.0117	0.9812	–0.20<x<0.20
4	10, 50	9.0–15.0	y=0.2613x–0.0065	0.9913	–0.20<x<0.20
Experiment 2: non-linear shear				0.9845	
1	16, 72	10.5–13.5	y=0.2064x^3–0.0937x^2+0.1506x+0.0004	0.9845	–0.30<x<0.30
2	16, 72	10.0–14.0	y=0.4174x^3–0.1081x^2+0.1558x+0.0013	0.9868	–0.30<x<0.30
3	17, 76	9.0–15.0	y=0.6591x^3–0.0641x^2+0.1914x+0.0009	0.9943	–0.30<x<0.30
4	13, 64	8.0–15.7	y=1.0302x^3–0.0953x^2+0.1107x+0.0025	0.9916	–0.30<x<0.30

x, displacement from the chamber center (center=0); y, vertical speed (cm s^{-1}).
All regressions were significant (P<0.05).

Regression of the tracer particles' velocities also yielded shear rate, the change in vertical flow velocity per unit horizontal distance across the chamber. In the initial experiments (total chamber breadth=0.7 cm), velocity regressions were linear across the central 0.4 cm of the chamber breadth (least-squares regression, R^2>0.98 in all cases; Table 3), indicating constant shear in that horizontal region. This meant that each temperature interval produced a different constant shear environment, and the effects of shear rate on swimming performance (speed and orientation) could be compared across treatments.

In the second set of experiments, ambient velocity in each treatment was best characterized by a cubic function of horizontal position, indicating a non-linear shear field. The first derivative of these velocity regressions (Table 3) yields 'instantaneous' shear for horizontal positions in these flow fields. Because embryos are not well approximated by dimensionless points, I calculated shear for each embryo position directly, by taking the velocity difference across the 160-μm diameter of a *D. excentricus* blastula.

RESULTS

Embryonic transport in turbulence

Developing motility did not change the direction of embryo transport in turbulence experiments, for either species examined. Upwelling flow was observed in recordings of turbulence. This is reflected in the distribution of mean-angle data for sampled intervals in both trials (Fig. 2A, Fig. 3A): in both unhatched (sinking) and swimming treatments, the mean trajectory was usually upwards. For *S. purpuratus*, there was no significant difference in mean angle ($\bar{a}$) between unhatched and swimming treatments (swimming: sin$\bar{a}$=0.126, cos$\bar{a}$=–0.002, R=0.126; unhatched: sin$\bar{a}$=0.041, cos$\bar{a}$=–0.024, R=0.047; Fig. 2B). This was also true for *D. excentricus* (swimming: sin$\bar{a}$=0.646, cos$\bar{a}$=0.220, R=0.682; unhatched: sin$\bar{a}$=0.368, cos$\bar{a}$=0.210, R=0.424; Fig. 3B). Retaining the anomalous downwelling samples in these tests increased the likelihood of detecting a difference between unhatched and swimming treatments. The result is therefore a robust indication that stage did not affect mean direction of transport.

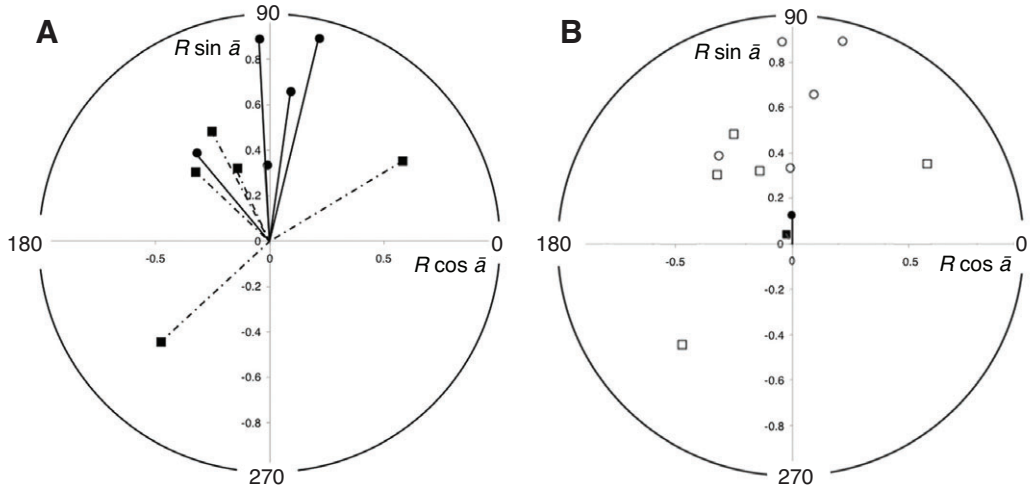

Fig. 2. Analysis of results for direction of embryo transport in turbulence. The Watson–Williams statistic for analysis of circular data (Zar, 1999) utilizes both the calculated mean angle for each sample ($\bar{a}$) and a variance measure that is expressed as a radius (R). The mean angle indicates a direction, whereas the lengths of mean-angle radii are inversely related to within-sample variance: a longer bar indicates lesser deviance in measures. (A) Plot of mean-angle results for *Strongylocentrotus purpuratus* transport during sampled intervals in turbulence-tank observations. Dashed bars/square markers represent samples from the recording with unhatched, non-motile blastulae. Each solid bar/circular marker represents one sample from the recording with swimming blastulae. The x- and y-axes are the horizontal and vertical directions. Bar angle indicates the mean trajectory (mean angle) of embryos' motion during the represented interval, and length is inversely proportional to sample variance. One-hundred and fifty embryos were measured in each of the five sampled intervals for each stage treatment. (B) Grand mean angles calculated for the Watson–Williams two-sample test for directional uniformity (n.s. difference between non-motile and swimming stages). The solid square/dashed line represents the grand mean angle from the recording with unhatched, nonmotile blastulae; the solid circle/solid line indicates the grand mean angle for swimming blastulae.

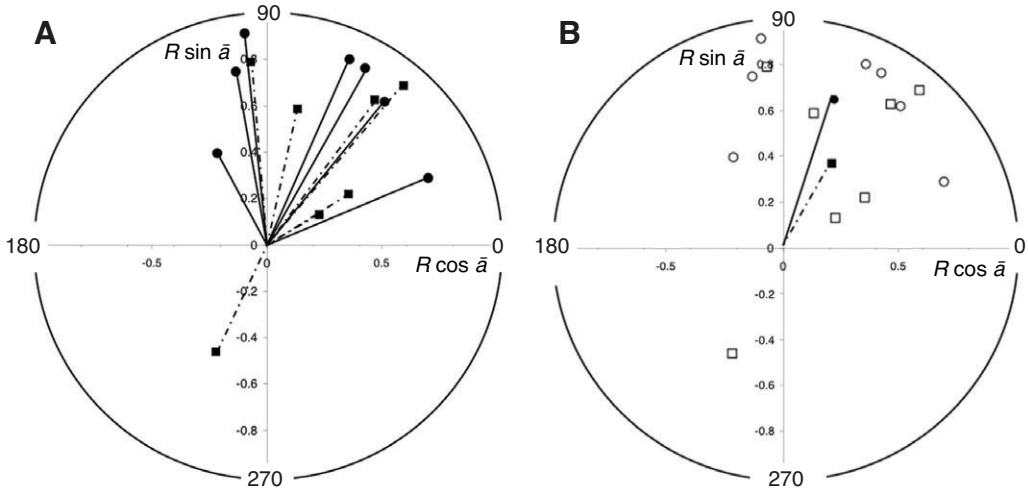

Fig. 3. (A) Plot of mean-angle results for motion of *D. excentricus* during subsampled intervals in turbulence-tank observations. All comments as for Fig. 2. One-hundred and twenty embryos were measured in each of the seven sampled intervals for each stage treatment. (B) Grand mean angles calculated for the Watson–Williams two-sample test (n.s. result). The solid square/dashed line represents the grand mean angle from the recording with unhatched, nonmotile blastulae; the solid circle/solid line indicates the grand mean angle for swimming blastulae.

Mean transport rates differed significantly with developmental stage (Table 2). The terms speed (magnitude of velocity) and velocity are used carefully: mean vertical velocity was calculated as a vector sum, with downward y-displacement signed negatively and upward y-displacement signed positively. For *S. purpuratus*, mean speed of motion was significantly greater in the swimming than in the unhatched treatment (P=0.011), but mean vertical velocity was greater (i.e. more positive) in the unhatched treatment (P<0.001). For *D. excentricus*, mean speed of motion was the same for unhatched and for swimming embryos (P=0.465), but mean vertical velocity was greater for swimmers (P<0.001).

Embryonic transport in linear shear

Experiments in linear shear located a 'turning point' for *D. excentricus* blastulae, defined as shear sufficient to turn swimming blastulae from their passive vertical orientation. Background flow-velocity regressions from tracer motion are reported in Table 3. In the first experiment, *D. excentricus* swimming blastulae maintained an upward orientation in constant shear of 0.229 to 0.248 s^{-1}, with variation generated in part by the helical swimming path that is characteristic at this stage (Fig. 4). At shear equal to 0.261 s^{-1}, swimming embryos were partially turned, so that their average orientation was approximately –0.6 rad from the vertical (Fig. 4). This is consistent with direct observation: in this shear treatment, embryos routinely crossed flow-lines, moving from upwelling into downwelling flow. In the circulation pattern induced in these experiments, with upwelling on the right, turning by shear resulted in a net leftward transport of embryos, hence the negative sign of the orientation angle (Fig. 4). Turning of swimmers was not observed in other shear treatments.

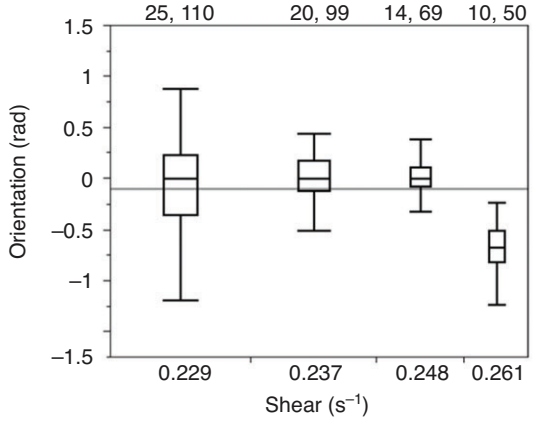

Fig. 4. Summary statistics for 1-s averaged orientation of *D. excentricus* swimming blastulae in four linear shear treatments. Mean orientation in radians from the vertical is plotted for each shear treatment, with box plots indicating 25th and 75th percentiles and bars indicating the data range. The number of embryos sampled and the number of total observations (embryos, observations) are reported for each shear treatment; in general, each embryo is represented by five haphazardly selected data for 1-s averaged orientation. A vertical orientation is y=0, a 90 deg leftward orientation is y=–π, and a 90 deg rightward orientation is y=π. In treatments 1–3, in which shear is lower (see Table 3), embryos maintained a mean vertical orientation (i.e. did not cross flow-lines). At a shear of 0.261 s^{-1} (treatment 4; see Table 3), embryos were turned to a mean angle of approximately –0.6 rad, and crossed into downwelling.

Prior to these experiments, it was assumed that the swimming speeds of blastulae were independent of shear. Contrary to expectation, instantaneous swimming speeds did vary with shear treatment (one-way ANOVA; total d.f.=327, F=80.7478, P<0.001). Fig. 5 shows summary statistics for swimming speed by treatment: swimming speeds in the shear range of 0.229–0.237 s^{-1} are lower than speeds measured in the shear range of 0.248–0.261 s^{-1}.

Embryonic transport in non-linear shear

These experiments were counterparts to the first set of experiments in shear. The use of a larger chamber had the advantage of allowing video-recording farther from the uncharacterized flow environment at the bottom. The increase in breadth also changed the shear field produced by temperature separation, so that background flow velocity was best characterized by a cubic rather than a linear function of horizontal position (Table 3). Because shears were non-linear (Fig. 6), embryos in different trials experienced similar shear, but at different locations; rates of change in shear varied with horizontal position within and across trials. This did not permit direct comparisons with the first experiment, but allowed me to examine the effects of shear and of variability in flow environment on swimming speed.

The flow environments experienced by embryos observed in these four treatments (Fig. 6) are compared in Fig. 7. Embryos were recorded while swimming in shears ranging from 0.150 to 0.275 s^{-1}. In treatments 1 and 4, the proportion of embryos recorded in each shear bin (increments of 0.025 s^{-1}) were similar; the same was true of treatments 2 and 3 (Fig. 7A). However, embryos in treatments 1 and 2 experienced only gentle gradients in shear, whereas those in treatments 3 and 4 experienced steep shear gradients (Fig. 7B). Because shear rates were lower, in general, than the 'turning point'

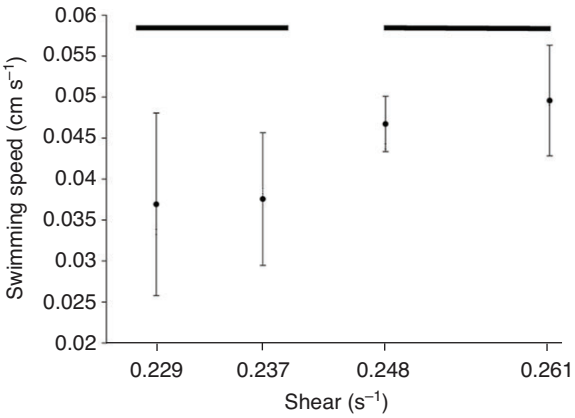

Fig. 5. Swimming speed of *D. excentricus* blastulae in four constant-shear treatments. Plot depicts mean ± s.d. swimming speed of blastulae in each treatment. Results of Tukey's honestly significant difference comparisons are shown above. Treatment effects on swimming speed were significant at $P<0.001$ (one-way ANOVA, JMP v. 6.0).

measured in the previous experiment (approximately $0.26\,s^{-1}$), embryos were not steadily crossing flow-lines. However, these blastulae could still sample variable flow conditions because of their helical swimming paths.

As in the first experiment, greater shear significantly increased *D. excentricus* swimming speed (Fig. 8). In treatments 1 and 2, where gradients in shear were lower, swimming speed showed a positive and significant relationship with shear (Fig. 8A,B). No significant relationship between shear and swimming speed was measured in treatment 3; in treatment 4, the relationship was significant, but explained little of the variance in speed (Fig. 8C,D). The weak responses in these latter two treatments seemed to result from highly variable swimming speeds where gradients (rates of change) in shear are high (Fig. 9). Where gradients in shear were highest, there also appeared to be deleterious effects on swimming speed itself (Fig. 9C).

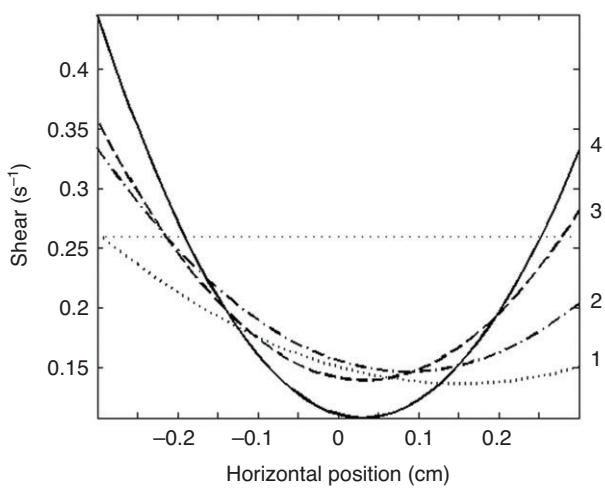

Fig. 6. Shear flow profiles across chamber breadth (plotted as distance x from chamber center) for experiments in non-linear shear. The horizontal interval depicted corresponds to the window of recorded observations; motion of embryos was analyzed within a smaller horizontal window ($-0.2\,cm<x<0.2\,cm$) because of high variability in swimming speeds in treatments 3 and 4 near the margins of the recording window. Treatments 1–4 are indicated at the right of the graph, and correspond to designations shown in Table 3. A dotted line at shear=$0.26\,s^{-1}$ indicates the projected point of turning for swimming blastulae of *D. excentricus*.

DISCUSSION

Results for velocities of *D. excentricus* blastulae in turbulence provide the first experimental evidence that benthic invertebrates can begin a planktonic migration when embryonic swimming commences. The transport consequences of upward swimming differed between *D. excentricus* and *S. purpuratus*, suggesting that interspecific differences in embryonic swimming velocity and passive stability may lead to different patterns of dispersal for early stages in nature.

For a passively stable motile embryo, upward swimming speed is a function of angle of orientation, with a coefficient set by total swimming speed. These studies of *D. excentricus* locate a 'turning-point' for stable swimming in shear, beyond which greater shear should produce greater average deviation from a vertical orientation. However, results also indicate that swimming speed is surprisingly responsive to velocity gradient. Upward transport is therefore turbulence dependent on two grounds: firstly because shear may turn the swimmer, and secondly because swimming speed itself changes with shear. The existence of swimming behavior even in earliest development means that generalizing transport consequences of swimming during development will require experimental observations of many more species, in addition to experimental or simulation-based investigation of the mechanisms of swimming enhancement. Predicting transport of planktonic embryos will require knowledge of species-specific coupling between the flow environment and swimming performance.

Swimming in turbulence

Results for vertical velocities of unhatched embryos and swimmers in turbulence indicate that swimming *D. excentricus* make an active contribution to their own upward transport where mean sub-microscale shear is on the order of $1\,s^{-1}$ (Table 1). However, swimming significantly impeded the upward transport of *S. purpuratus* in turbulence: although they were moving faster, swimming blastulae were also moving downward relative to unhatched stages.

Different consequences of hatching for transport could arise in part from interspecific differences in embryonic stability. Blastulae of both species are nearly spherical at hatching. Although *S. purpuratus* blastulae have approximately twice the excess density of blastulae of *D. excentricus* (data calculated from embryonic sinking speeds in still water) (McDonald, 2004), they also have a much smaller radius (approximately 50 μm, as compared with 75–80 μm). The magnitude of a blastula's passive stabilizing moment is proportional to its density, as well as to the distance separating its centers of buoyancy and gravity, which can be taken as proportional to the radius in these coeloblastulae (Grünbaum and Strathmann, 2003; Mogami et al., 2001) (see Eqn 1). If the moment force exerted by flow on the swimmer (see Eqn 2) exceeds the body-force moment that generates passive stability, the swimmer is rotated. We can therefore compare the relative resistance to turning of isometric embryos with similar ciliation by using the dimensionless expression:

$$\frac{r\left[\rho \boldsymbol{g} r^3\right]}{r\left[\boldsymbol{\nabla}\mathbf{U}\mu r^2\right]}\,, \tag{3}$$

which simplifies to:

$$\frac{\rho \boldsymbol{g} r}{\boldsymbol{\nabla}\mathbf{U}\mu}\,. \tag{4}$$

Because their differences in excess density and size are in counterpoise, *D. excentricus* and *S. purpuratus* blastulae should

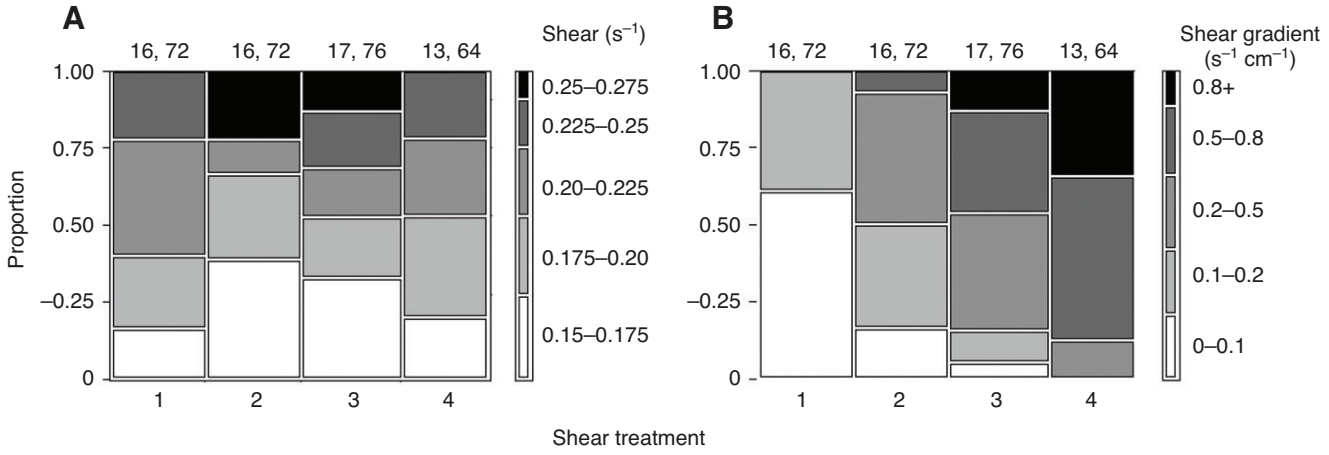

Fig. 7. Shear- and shear-gradient distributions for observations made in non-linear shear treatments 1–4. See Table 3 and Fig. 6 for regressions and shear profiles for these treatments. The number of embryos sampled and the number of total observations (embryos, observations) are reported for each shear treatment; in general, each embryo is represented by five haphazardly selected data for 1-s averaged orientation. Some data were trimmed for embryos swimming near the margins of the observation window. (A) In treatments 1 and 4, the proportion of embryos recorded in each shear bin (increments of 0.025 s^{-1}) were similar; the same was true of treatments 2 and 3. Only in treatments 2 and 3 were measures made in shears of 0.25–0.275 s^{-1}. (B) Embryos in treatments 1 and 2 experienced only gentle gradients in shear, whereas those in treatments 3 and 4 experienced steeper shear gradients.

show similar passive stability in shear flow; *S. purpuratus* may be slightly more stable, as its excess density is twice that of *D. excentricus*, whereas its radius is greater than one-half that of *D. excentricus*. It follows that differences in transport outcomes of swimming in turbulence cannot be attributed to an obvious difference in passive stability.

If *S. purpuratus* possesses the same or slightly greater passive stability than *D. excentricus* blastulae, then it is likely then that swimmers of both species were turned from their passive, vertical orientations in these experiments. The microscale of shear was on the order of 1 s^{-1} (Table 1), and results of experiments in constant shear indicate that *D. excentricus* blastulae are turned from the vertical when shear approaches 0.26 s^{-1}. Because the turning by shear of a passively stable swimmer is biased toward downwelling, any change in orientation increases the probability of transport into transient downwelling. This effect is heightened by increases in swimming speed; embryos will cross flow-lines faster. *Strongylocentrotus purpuratus* has a still-water swimming speed of 0.45 mm s^{-1}, compared with 0.22 mm s^{-1} in *D. excentricus* (measured at 10°C) (McDonald, 2004). This considerable difference in swimming speed at time of hatching likely contributed to the difference in the effect of swimming on their rates of upward transport in turbulence.

Results for vertical velocity and total speed of transport suggest that interspecific differences in embryo size and swimming speed could contribute to differences in the ecology of planktonic embryos. Turbulence that permits upward migration in early development for one echinoid species may cause the same stage in a related species to migrate downward, or it may reduce the upward transport that would result if embryos simply hatched at a later stage in development. Early swimming speeds may scale strongly with size in echinoids, with upward swimming speeds of smaller embryos significantly greater than speeds of larger embryos in a sample of northeastern Pacific species (McDonald, 2004). If greater speed is not counterbalanced by greater passive stability, then one might anticipate a size dependency in the vertical distribution of planktonic embryos of different echinoid species. Size-dependent swimming performance would provide an alternative perspective on the role of egg size in development. Egg size is usually regarded as a proxy for nutritional content, as evolutionary changes in egg size are correlated with changes in mode of development (i.e. increased egg size indicates a shift away from planktotrophy). These and other studies of swimming embryos indicate that egg size could influence embryonic ecology, and therefore the evolution of development, *via* transport processes as well as nutritional mode (McDonald and Grünbaum, 2010).

Assessing the full effects of interspecific differences in embryonic speed and stability on transport also requires knowledge of adult ecology and water-column structure. Embryos of broadcast-spawning species, such as these echinoderms, are mixed into different turbulence regimes depending upon parental habitat. Embryos from species spawning at depth may not encounter turbulence of the intensity employed in this study until later in development, when they have very different forms, whereas embryos of shallow-water species will contend with similar turbulence from the time they become motile. There could be a relationship between spawning habitat or depth and early embryonic swimming performance. In red abalone (*Haliotis rufescens*), for example, optimum swimming speed and fertilization success for sperm are achieved in flow conditions similar to those that characterize adult microhabitats (Riffell and Zimmer, 2007). However, early embryos are likely to be dispersed away from the immediate vicinity of adult spawning grounds by the time they become motile (on the order of 20 h after fertilization for temperate echinoderms) (e.g. Staver and Strathmann, 2002), so differences in species' depth distributions may be more relevant to the question of adaptive differences in swimming performance. *Strongylocentrotus purpuratus* and *D. excentricus* do occupy quite different habitat types as adults, but both species are common at shallow depths (<30 m).

Transport upwards and into warmer layers, where development times are shorter and food is more abundant, would seem an optimal outcome of swimming in planktotrophs. However, early characteristics of speed and stability are transitional. Embryos change in aspect and often ciliation pattern, and as they gastrulate

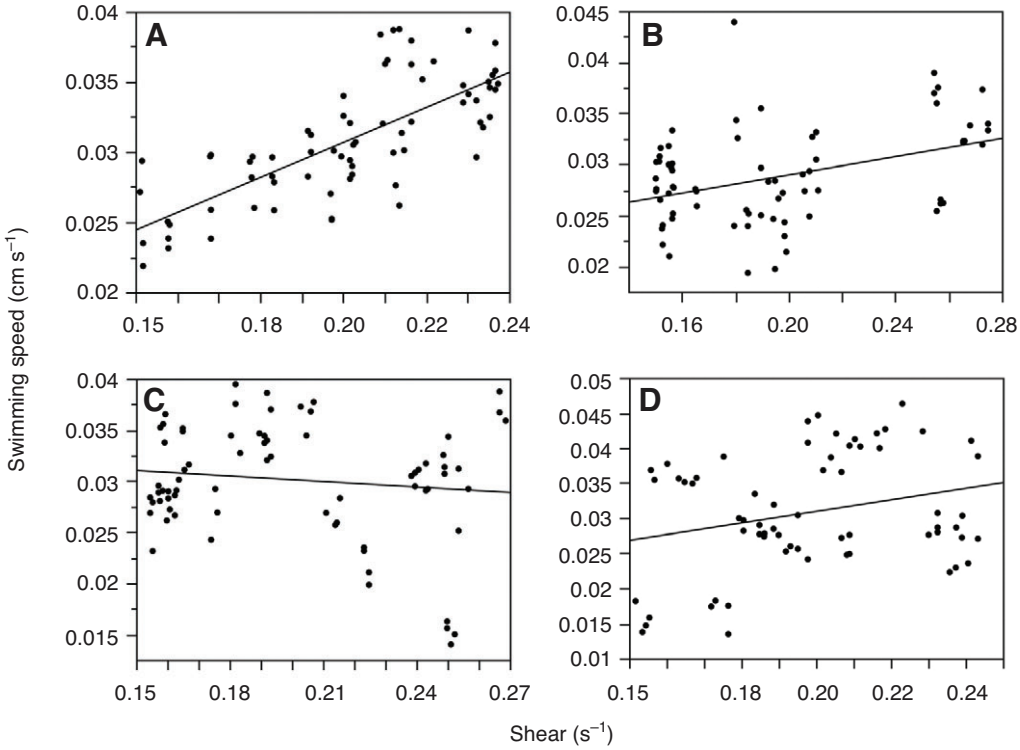

Fig. 8. Swimming speeds of *D. excentricus* blastulae in four non-linear shear treatments. One-second averaged speed, with background flow subtracted, is plotted against shear rate. For treatment designations, see Table 3; for shear profiles by treatment, see Fig. 6. The distribution of embryos observed at different levels of shear is shown for each treatment in Fig. 7. Regressions were significant for treatments 1, 2 and 4. In those treatments, swimming speeds showed a positive correlation with shear. (A) Treatment 1 swimming speed regression: speed=0.00569+0.125(shear); R^2= 0.550, N=72 observations, P<0.0001. (B) Treatment 2 swimming speed regression: speed=0.0200+0.0445(shear); R^2= 0.153, N=72 observations, P=0.0007. (C) Treatment 3 swimming speed regression: speed=0.0337–0.0179(shear); R^2= 0.0148, N=76 observations, P=0.295. (D) Treatment 4 swimming speed regression: speed=0.0145+0.0822(shear); R^2= 0.0699, N=64 observations, P=0.0347.

their buoyancy may also alter. The most critical and general consequence of first swimming may be prevention of an early and disadvantageous return to the near-bottom environment.

Swimming in linear and non-linear shear

All experiments with shear simulated a flow environment that embryos encounter in low to moderate coastal turbulence (ε=10^{-4}–10^{-3} cm^2 s^{-3} or 10^{-8}–10^{-7} W kg^{-1}; Table 3). A 'turning-point' in the vicinity of 0.25–0.26 s^{-1} indicates that, on average, *D. excentricus* swimming blastulae will remain vertically oriented until energy dissipation rates approach 10^{-3} cm^2 s^{-3}. That early ciliary swimming provides some effective upward transport beyond this point is indicated by results from the experiment of *D. excentricus* blastulae swimming in turbulence, where energy dissipation was estimated at an order of magnitude higher. These results in laminar shear demonstrate that newly hatched *D. excentricus* blastulae do possess swimming stability under conditions they are likely to experience in nature.

Effects of shear on swimming speed were significant. Within the range of shear tested, greater shear significantly increased embryonic swimming speed (Figs 5, 8). The four non-linear shear treatments (Table 3, Fig. 6) overlapped in range of shear, but differed in rates of change in shear (Figs 6, 7). In addition to demonstrating a positive effect of shear on swimming speed, experimental results indicated that this effect was greater in treatments where the rate of change in shear (i.e. change in flow-velocity differential across the embryo per unit horizontal distance) was lower.

Different shear gradients may have led to differences in swimmers' experience. Echinoid blastulae swim in a helix of variable pitch; as embryos swim upwards, their experience of shear may remain constant, as in the linear shear fields of the first experiment, or it may change during the course of each horizontal excursion. In a steeply changing velocity gradient, these periodic horizontal excursions will result in a highly variable experience of shear, which could complicate ciliary coordination and reduce consistency in swimming speed, or disrupt swimming altogether. A relatively constant velocity gradient could minimize disruptions to swimming and result in more consistent swimming speeds.

A single mechanism might be responsible for shear effects on swimming speed and consistency. One hypothesis is that steep velocity gradients alter ciliary dynamics for these continuously ciliated embryos, increasing the power generated by individual cilia or increasing overall propulsive efficiency. With increasing shear, however, ciliary coordination (the coupling of recovery strokes among neighboring cilia) may be increasingly disrupted, resulting in variable performance and failure of swimming at sufficiently high shear. Beat pattern could also alter across the organism, with consequences for pitch of the swimming helix and, therefore, the rate of upward translation. If a limited disruption of ciliary coupling (e.g. Brennan, 1975; Blake and Sleigh, 1975) allows swimmers to attain greater speeds in moderate shear, swimming enhancement should be limited to a range of shear determined by the mechanical properties of the cilia, their length and spacing, and the curvature of the ciliated surface.

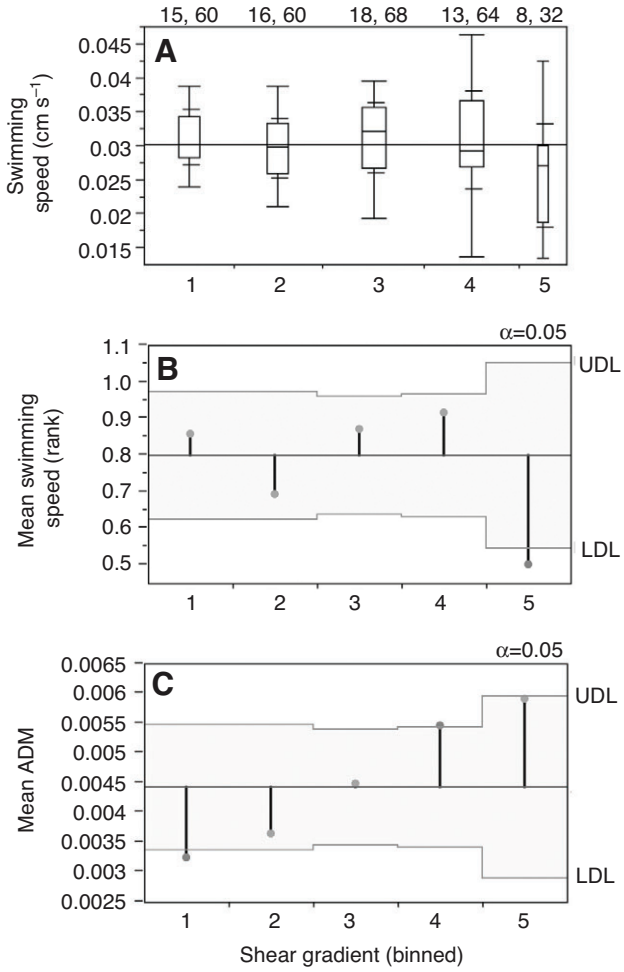

Fig. 9. Effects of shear gradient on the swimming speed of *D. excentricus* blastulae in non-linear shear treatments. Even when shear itself is gentle (see Fig. 7), steeper changes in shear appear to have deleterious effects on swimming speed and consistency. This suggests that rapid changes in flow environment, even in gentle flow, may transiently disrupt ciliary coordination. (A) Box plots for swimming speed data from all treatments, binned by shear gradient (rate of change in shear per unit horizontal distance). Shear gradient bins are as shown in Fig. 7. Box plots indicate 25th and 75th data percentiles and range, and bars indicate ±s.d. The number of embryos sampled and the number of total observations (embryos, observations) in each bin are reported. Several embryos contributed observations to more than one bin, and thus are counted in each. (B) Analysis of means (each group mean tested against the whole-sample mean; JMP v. 9.0) using transformed ranks indicates that the mean swimming speed in the highest shear-gradient bin was significantly lower than the whole-sample mean ($P<0.05$). LDL, lower decision limit; UDL, upper decision limit. (C) Analysis of means for variance (the ANOM version of Levene's test; JMP v. 9.0) supports the observation that lower gradients in shear are associated with more consistent, less variable swimming speeds, while higher gradients result in greater variance in swimming speed. Mean variance increases across shear-gradient bins: the lowest bin shows significantly below-average variance in speed, and the highest bins show significant and near-significant increases in variance compared with the whole-sample mean of absolute deviations from the median (ADM).

Shear should have significant effects on swimming speed in a range of ciliated and flagellated planktonic organisms if the mechanism of swimming enhancement acts at the level of ciliary or flagellar coordination, or predictably affects the function of individual organelles. Chain-forming dinoflagellates demonstrate higher swimming speeds in laminar shear on the order of $1\,s^{-1}$ (Karp-Boss et al., 2000), similar to the sub-microscale shear conditions estimated for the turbulence that echinoid embryos experienced in this study. In addition, low shear ($0.1\,s^{-1}$) has been shown to enhance swimming speed in *H. rufescens* sperm, whereas higher levels of shear ($0.5\,s^{-1}$ and greater) reduced swimming speed (Riffell and Zimmer, 2007).

Ecologically, optimal swimming performance may not be defined by speed. If moving upwards is beneficial for early embryos, then faster swimming could be useful, but the adaptive value of speed would diminish if it facilitated transport into downwelling over a range of commonly encountered energetic conditions. Variability in swimming speed observed at higher shear and in steeper shear gradients (Figs 8, 9) may also have consequences for cohort vertical distribution. Stronger and more variable swimming performance in high-energy conditions will enhance spatial dispersal by contributing to physical diffusion, so that the vertical extent of dispersal could be greater because of swimming.

This discussion has focused on the interactions between flow environment and embryonic behavior that influence vertical migration. The near-ubiquity of rapid development to motility among broadcast-spawning invertebrates raises the question of the adaptive value of swimming in early development. Considering the simplicity of the study organisms, upward swimming may have surprisingly complex consequences for migration, but migration in the plankton is only one possible outcome of swimming. The results of *in situ* experiments with advanced larval stages support the long-standing hypothesis that unprotected benthic development carries greater predation risk (e.g. Allen and McAlister, 2007). The results reported here demonstrate that swimming at the time when embryos first become motile could effect transport away from the benthos. If swimming moves the most vulnerable developmental stages to safer depths, then that fundamental consequence of motility may explain the importance of rapid development of ciliary swimming in the evolution of planktonic development.

LIST OF SYMBOLS

g	constant of gravitational acceleration
$\mathbf{M_B}$	stabilizing moment from body forces
$\mathbf{M_S}$	stabilizing moment from external flow
r	radius
$\mathbf{U}$	flow speed
v	Kolmogorov velocity, or mean velocity below Kolmogorov length (η)
ε	rate of turbulent kinetic energy dissipation
ρ	excess density
μ	dynamic viscosity
η	Kolmogorov length, or microscale of turbulence

ACKNOWLEDGEMENTS

Many thanks to Richard R. Strathmann and Danny Grünbaum for advice and discussion during all stages of this project. Rachel Collin, Kecia Kerr and Maryna Lesoway provided constructive criticism on this manuscript. I thank my graduate advisory committee (Richard R. Strathmann, Danny Grünbaum, Tom Daniel and Jennifer Ruesink) for their suggestions and support, and Tansy Clay for many helpful discussions of the impacts of growth form on larval transport. Liko Self drew my attention to the turbulence tank as a research tool. I am grateful to the stimulating scientific communities of the Friday Harbor Laboratories and the Smithsonian Tropical Research Institute.

FUNDING

This work was supported by National Science Foundation [grant OCE-0217304 to R. R. Strathmann], and by a Wainwright Fellowship from the Friday Harbor Laboratories.

REFERENCES

Allen, J. D. and McAlister, J. S. (2007). Testing rates of planktonic versus benthic predation in the field. *J. Exp. Mar. Biol. Ecol.* **347**, 77-87.

Bearon, R. N., Grünbaum, D. and Cattolico, R. A. (2004). Relating cell-level swimming behaviors to vertical population distributions in *Heterosigma akashiwo* (Raphidophyceae), a harmful alga. *Limnol. Oceanogr.* **49**, 607-613.

Bearon, R. N., Grünbaum, D. and Cattolico, R. A. (2006). Effects of salinity structure on swimming behavior and harmful algal bloom formation in *Heterosigma akashiwo*, a toxic raphidophyte. *Mar. Ecol. Prog. Ser.* **306**, 153-163.

Blake, J. R. and Sleigh, M. A. (1975). Hydromechanical aspects of ciliary propulsion. In *Swimming and Flying in Nature*, Vol. 1 (ed. T. Y. Wu, C. J. Brokaw and C. Brennan), pp. 185-209. New York: Plenum.

Bollens, S. M., Frost, B. W., Thoreson, D. S. and Watts, S. J. (2002). Diel vertical migration in zooplankton: field evidence in support of the predator avoidance hypothesis. *Hydrobiologia* **1**, 33-39.

Bollens, S. M., Rollwagen-Bollens, G., Quenette, J. A. and Bochdansky, A. B. (2011). Cascading migrations and implications for vertical fluxes in pelagic ecosystems. *J. Plankton Res.* **33**, 349-355.

Brennan, C. (1975). Hydromechanics of propulsion for ciliated microorganisms. In *Swimming and Flying in Nature*, Vol. 1 (ed. T. Y. Wu, C. J. Brokaw and C. Brennan), pp. 235-251. New York: Plenum.

Brumley, B. H. and Jirka, G. H. (1987). Near-surface turbulence in a grid-stirred tank. *J. Fluid. Mech.* **183**, 235-263.

Chan, K. Y. K. and Grünbaum, D. (2010). Temperature and diet modified swimming behaviors of larval sand dollar. *Mar. Ecol. Prog. Ser.* **415**, 49-59.

Childress, J. J. and Nygaard, M. (1974). Chemical composition and buoyancy of midwater crustaceans as a function of depth of occurrence off southern California. *Mar. Biol.* **27**, 225-238.

Clay, T. and Grünbaum, D. (2010). Morphology-flow interactions lead to stage-specific vertical transport of larval sand dollars in shear flow. *J. Exp. Biol.* **213**, 1281-1292.

Clay, T. and Grünbaum, D. (2011). Swimming performance as a constraint on larval morphology in plutei. *Mar. Ecol. Prog. Ser.* **423**, 185-196.

Coombs, S. H., Fosh, C. A. and Keen, M. A. (1985). The buoyancy and vertical distribution of eggs of sprat (*Sprattus sprattus*) and pilchard (*Sardina pilchardus*). *J. Mar. Biol. Assoc. UK* **65**, 461-474.

Emlet, R. B. (1986). Larval production, dispersal, and growth in a fjord: a case study on larvae of the sand dollar *Dendraster excentricus*. *Mar. Ecol. Prog. Ser.* **31**, 245-254.

Fuchs, H. L., Mullineaux, L. S. and Solow, A. R. (2004). Sinking behavior of gastropod larvae (*Ilyanassa obsoleta*) in turbulence. *Limnol. Oceanogr.* **49**, 1937-1948.

Fuchs, H. L., Neubert, M. G. and Mullineaux, L. S. (2007). Effects of turbulence-mediated larval behavior on larval supply and settlement in tidal currents. *Limnol. Oceanogr.* **52**, 1156-1165.

Fuchs, H. L., Solow, A. R. and Mullineaux, L. S. (2010). Larval responses to turbulence and temperature in a tidal inlet: habitat selection by dispersing gastropods? *J. Mar. Res.* **68**, 153-188.

Gallager, S. M. (1993). Hydrodynamic disturbances produced by small zooplankton: case study for the veliger larva of a bivalve mollusc. *J. Plankton Res.* **15**, 1277-1296.

Gargett, A. E. (1984). Vertical eddy diffusivity in the ocean interior. *J. Mar. Res.* **42**, 359-395.

Garland, E. D., Zimmer, C. A. and Lentz, S. J. (2002). Larval distributions in inner-shelf waters: the roles of wind-driven cross-shelf currents and diel vertical migrations. *Limnol. Oceanogr.* **47**, 803-817.

George, R., Flick, R. T. and Guza, R. T. (1994). Observations of turbulence in the surf zone. *J. Geophys. Res.* **99**, 801-810.

Grünbaum, D. and Strathmann, R. R. (2003). Form, performance, and trade-offs in swimming and stability of armed larvae. *J. Mar. Res.* **61**, 659-691.

Hill, P. S., Nowell, A. R. S. and Jumars, P. A. (1992). Encounter rate by turbulent shear of particles similar in diameter to the Kolmogorov scale. *J. Mar. Res.* **50**, 643-668.

Kamykowski, D. and Yamazaki, H. (1997). A study of metabolism-influenced orientation in the diel vertical migration of marine dinoflagellates. *Limnol. Oceanogr.* **42**, 1189-1202.

Karp-Boss, L., Boss, E. and Jumars, P. A. (2000). Motion of dinoflagellates in a simple shear flow. *Limnol. Oceanogr.* **45**, 1594-1602.

Kelman, D. and Emlet, R. B. (1999). Swimming and buoyancy in ontogenetic stages of the cushion star *Pteraster tesselatus* (Echinodermata: Asteroidea) and their implications for distribution and movement. *Biol. Bull.* **197**, 309-314.

Koehl, M. A. R., Strother, J. A., Reidenbach, M. A., Koseff, J. R. and Hadfield, M. G. (2007). Individual-based model of larval transport to coral reefs in turbulent, wave-driven flow: behavioral responses to dissolved settlement inducer. *Mar. Ecol. Prog. Ser.* **335**, 1-18.

Lampert, W. (1989). The adaptive significance of diel vertical migration of zooplankton. *Funct. Ecol.* **3**, 21-27.

Marra, J. (1980). Time-course of light intensity adaptation in a marine diatom. *Mar. Biol. Lett.* **1**, 175-180.

Marta-Almeida, M., Dubert, J., Peliz, A. and Queiroga, H. (2006). Influence of vertical migration pattern on retention of crab larvae in a seasonal upwelling system. *Mar. Ecol. Prog. Ser.* **307**, 1-19.

McDonald, K. (2004). Patterns in early embryonic motility: effects of size and environmental temperature on vertical velocities of sinking and swimming echinoid blastulae. *Biol. Bull.* **207**, 93-102.

McDonald, K. A. and Grünbaum, D. (2010). Swimming performance in early development and the "other" consequences of egg size for ciliated planktonic larvae. *Integr. Comp. Biol.* **50**, 589-605.

McKenzie, B. R. and Leggett, W. C. (1993). Wind-based models for estimating the dissipation rates of turbulent energy in aquatic environments: empirical comparisons. *Mar. Ecol. Prog. Ser.* **94**, 207-216.

Medeiros-Bergen, D. E., Olson, R. R., Conroy, J. A. and Kocher, T. D. (1995). Distribution of holothurian larvae determined with species-specific genetic probes. *Limnol. Oceanogr.* **40**, 1225-1235.

Metaxas, A. (2001). Behaviour in flow: perspectives on the distribution and dispersion of meroplanktonic larvae in the water column. *Can. J. Fish. Aquat. Sci.* **58**, 86-98.

Mogami, Y., Ishii, J. and Baba, S. A. (2001). Theoretical and experimental dissection of gravity-dependent mechanical orientation in gravitactic microorganisms. *Biol. Bull.* **201**, 26-33.

Morgan, S. G. (1990). Impact of planktivorous fishes on dispersal, hatching, and morphology of estuarine crab larvae. *Ecology* **71**, 1639-1652.

Oakey, N. S. and Elliot, J. A. (1982). Dissipation within the surface mixed layer. *J. Phys. Oceanogr.* **12**, 171-185.

Podolsky, R. D. (1995). Consequences of temperature, viscosity, and small size for early life-history processes in the sand dollar *Dendraster excentricus*. PhD dissertation, University of Washington, Seattle, WA, USA.

Poulin, E., Palma, A. T., Leiva, G., Narvaez, D., Pacheco, R., Navarrete, S. A. and Castilla, J. C. (2002). Avoiding offshore transport of competent larvae during upwelling events: the case of the gastropod *Concholepas concholepas* in central Chile. *Limnol. Ocean.* **47**, 1248-1255.

Prézelin, B. B. (1992). Diel periodicity in phytoplankton productivity. *Hydrobiologia* **238**, 1-35.

Riffell, J. A. and Zimmer, R. K. (2007). Sex and flow: the consequences of fluid shear for sperm–egg interactions. *J. Exp. Biol.* **210**, 3644-3660.

Seuront, L., Yamazaki, H. and Souissi, S. (2004). Hydrodynamic disturbance and zooplankton swimming behavior. *Zool. Stud.* **43**, 376-387.

Shanks, A. L. (1985). Behavioural basis of internal-wave induced shoreward transport of megalopae of the crab *Pachygrapsus crassipes*. *Mar. Ecol. Prog. Ser.* **24**, 289-295.

Staver, J. H. and Strathmann, R. R. (2002). Evolution of fast development of planktonic embryos to early swimming. *Biol. Bull.* **203**, 58-69.

Strathmann, M. (1987). *Reproduction and Development of Marine Invertebrates of the Northern Pacific Coast.* Seattle, WA: University of Washington Press.

Strathmann, R. R. (1982). Selection for retention or export of larvae in estuaries. In *Estuarine Comparisons* (ed. V. S. Kennedy), pp. 521-536. New York: Academic Press.

Sundby, S. (1983). A one-dimensional model for the vertical distribution of pelagic fish eggs in the mixed layer. *Deep Sea Res.* **30**, 645-661.

Sundby, S. (1997). Turbulence and icthyoplankton: influence on vertical distribution and encounter rates. *Sci. Mar.* **61, Suppl. 1**, 159-176.

Verdier-Bonnet, C., Carlotti, F., Rey, C. and Bhaud, M. (1997). A model of larval dispersion coupling coupling wind-driven currents and vertical larval behaviour: application to the recruitment of the annelid *Owenia fusiformis* in Banyuls Bay, France. *Mar. Ecol. Prog. Ser.* **160**, 217-231.

Visser, A. W. and Jonasdóttir, S. H. (1999). Lipids, buoyancy, and the seasonal vertical migration of *Calanus finmarchicus*. *Fish. Oceanogr.* **8 Suppl. 1**, 100-106.

Yamazaki, H. and Squires, K. D. (1996). Comparison of oceanic turbulence and copepod swimming. *Mar. Ecol. Prog. Ser.* **144**, 299-301.

Yamazaki, H., Mackas, D. L. and Denman, K. L. (2002). Coupling small-scale physical processes with biology. In *The Sea*, Vol. 12, *Biological-physical interactions in the sea* (ed. A. R. Robinson, J. J. McCarthy and B. J. Rothschild), pp. 51-112. New York: Wiley and Sons.

Young, C. M. (1995). Behavior and locomotion during the dispersal phase of larval life. In *Ecology of Marine Invertebrate Larvae* (ed. L. McEdward), pp. 247-277. Boca Raton, FL: CRC Press.

Young, C. M. and Cameron, J. L. (1987). Laboratory and *in situ* floating rates of lecithotrophic eggs from the bathyal echinoid *Phormosoma placenta*. *Deep Sea Res.* **34**, 1629-1639.

Young, C. M. and Chia, F.-S. (1987). Abundance and distribution of pelagic larvae as influenced by predation, behavior, and hydrographic factors. In *Reproduction of Marine Invertebrates*, Vol. 9 (ed. A. C. Giese, J. S. Pearse and V. B. Pearse), pp. 385-463. Palo Alto, CA: Blackwell Scientific.

Zar, J. (1999). *Biostatistical Analysis*, 4th edn. Upper Saddle River, NJ: Prentice Hall.